RESEARCH ARTICLE

Figures and figure supplements

Organelle calcium-derived voltage oscillations in pacemaker neurons drive the motor program for food-seeking behavior in *Aplysia*

Alexis Bédécarrats *et al*

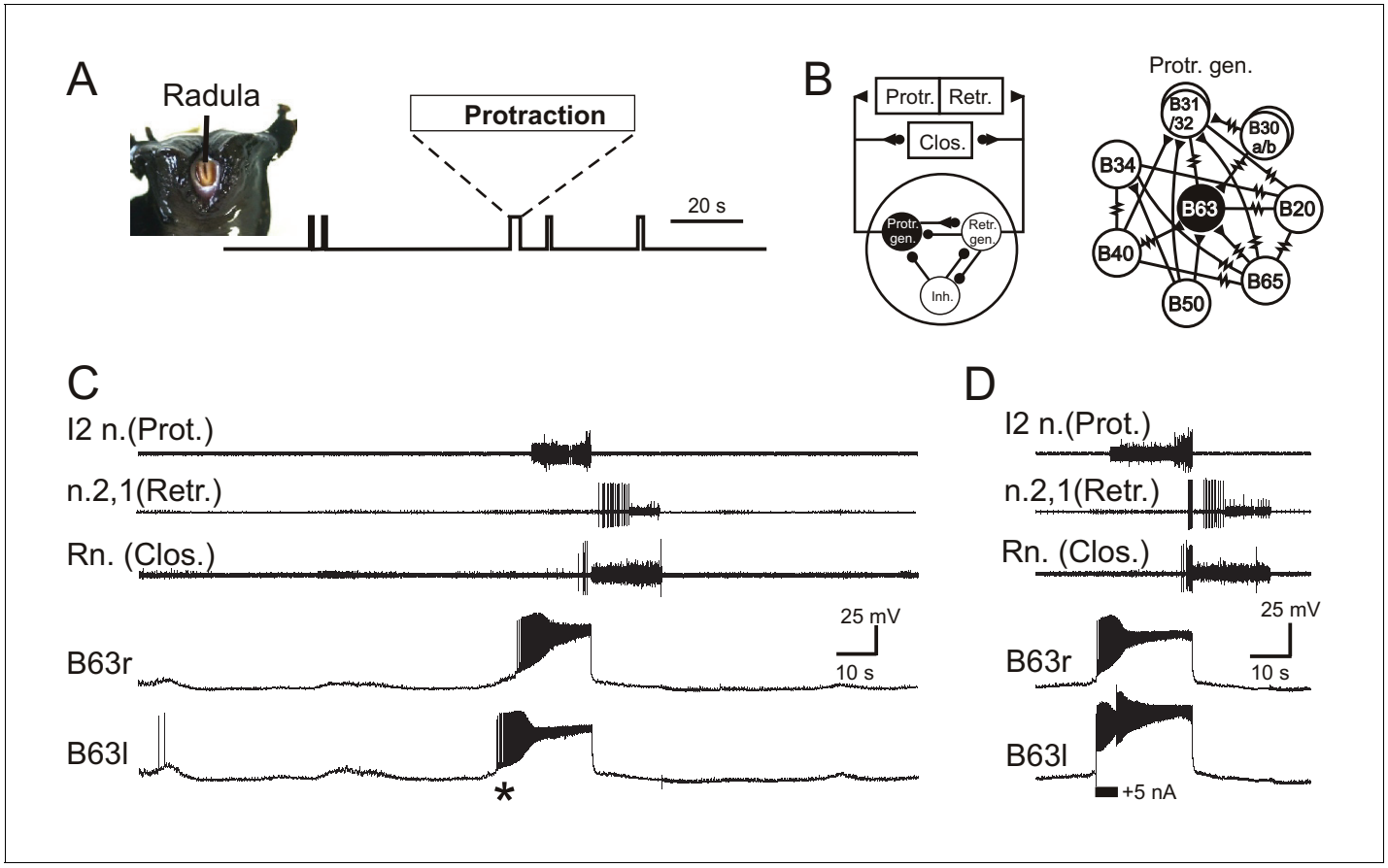

Figure 1. *Aplysia*'s spontaneous radula biting behavior and underlying motor pattern generation. (**A**) In vivo food-seeking behavior. In the absence of any external stimulation, *Aplysia's* radula (see head frontal view at left) spontaneously produces biting movements consisting of irregularly timed cycles of radula protraction (upward deflection of movement monitor trace), closure and retraction (downward deflection). (**B**) Schematics of the buccal CPG network that generates radula biting movements. Left: simplified diagram of the half-center network (one in each of the bilateral buccal ganglia) and its synaptic connections with protraction (Protr.), retraction (Retr.) and closure (Clos.) motoneurons (filled circles and triangles; inhibitory and excitatory connections, respectively). The network producing each bi-phasic cycle of movement is composed of three distinct and synaptically connected neuronal subsets comprising a protraction generator (Protr. gen.), a retraction generator (Retr. gen.) and a group of inhibitory neurons (Inh.). Right: detailed schematic of identified neurons belonging to the protraction generator and their synaptic interconnections (filled triangles, excitatory chemical synapses; resistance symbols, electrical synapses). Within the protraction generator, the neuron B63 (black) is necessary and sufficient to trigger the buccal motor pattern (BMP) for a radula bite cycle. (**C**) Simultaneous extracellular recordings of a single BMP (top three traces) and intracellular recordings of the two bilateral and electrically-coupled B63 neurons (r, right; l, left) in an isolated in vitro buccal ganglia preparation. I2n., n.2,1, Rn., are respectively the motor nerves carrying axons of protractor, retractor and closure motor neurons. The two B63 cells expressed spontaneous and coincident membrane depolarizations (*) that initiated plateau potentials and associated impulse bursts, which in turn evoked a BMP by the buccal CPG network. (**D**) Synchronous plateau potentials in the electrically coupled B63 and a resulting BMP triggered by a brief intracellular depolarizing current pulse (+5 nA) injected into one (left) B63 neuron.

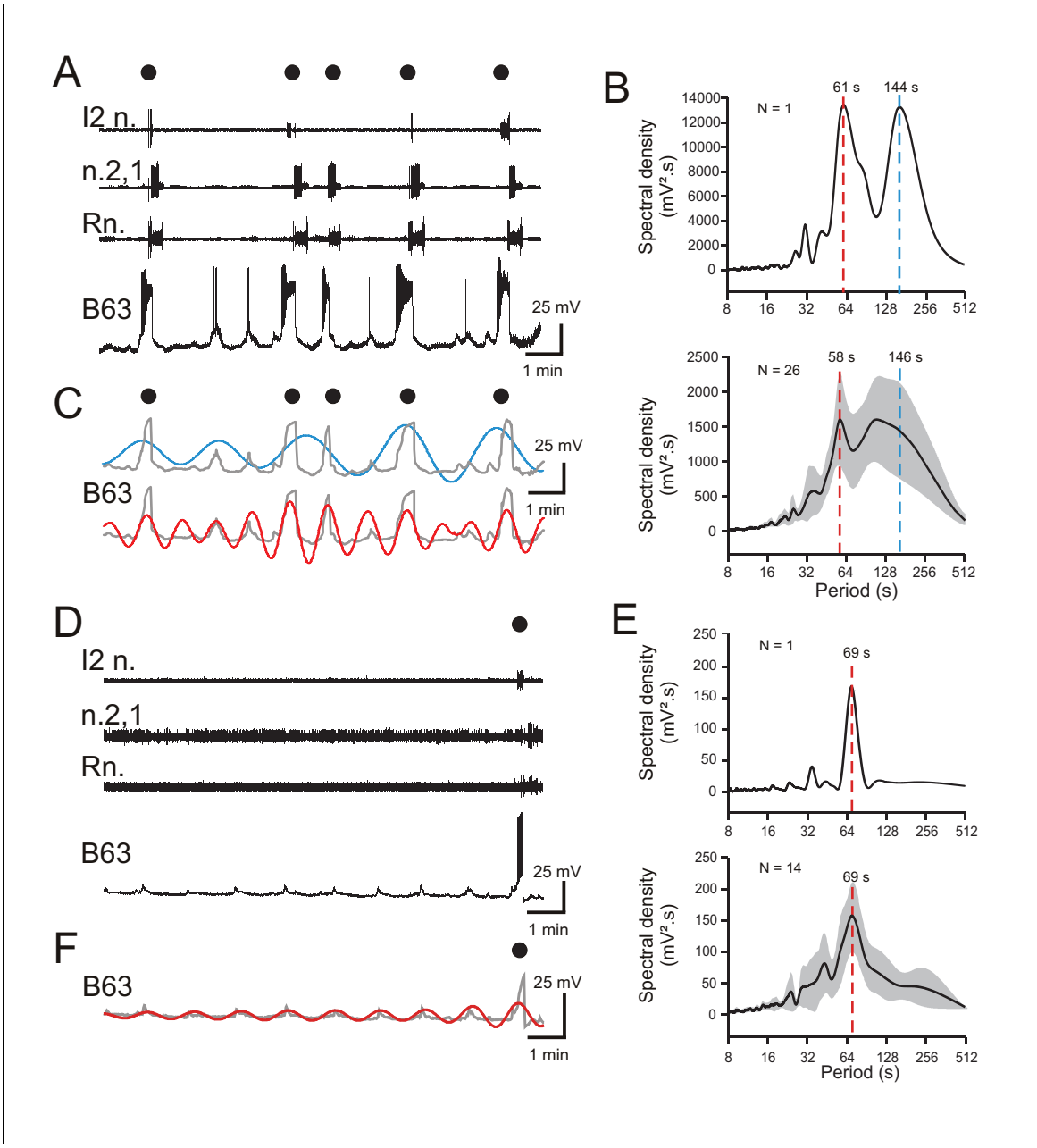

Figure 2. Periodicities in B63's spontaneous bioelectrical behavior. (**A**) A 10 min recording excerpt of radula BMP genesis (black dots) in an in vitro buccal ganglion preparation showing associated spontaneous fluctuations in membrane potential of an intracellularly recorded B63 neuron. Note that a BMP occurred only when B63 expressed prolonged burst firing driven by a plateau potential. (**B**) Spectral density plot of the B63 recording illustrated in A (top) and the average power spectrum (± CI95%) from recordings of 26 different neurons (bottom). In both cases, the essentially bimodal periodograms indicated that the variations in B63's membrane potential comprised two distinct periodicities (red and blue dashed lines indicate the means of these two dominant periods rather than peaks of average power), which across all 26 neurons was 58 s and 146 s, respectively. For details see ***Figure 2—figure supplement 1A***. (**C**) Wavelet-based reconstructions retaining the two dominant periods revealed in the individual power spectrum in B (top) and their superposition with the smoothed membrane voltage traces (gray) of the corresponding B63 neuron in A. The slower sinusoid (blue trace; period, 144 s) corresponded to the cell's strongest depolarizations associated exclusively with the expression of plateau potentials and resultant BMP genesis (black dots). The faster sinusoid (red trace; period, 61 s) corresponded to these supra-threshold depolarizations plus almost all remaining subthreshold depolarizations. (**D–F**) Equivalent analyses of the same neurons as in **A-C**, but during recorded excerpts when no plateauing and BMP genesis occurred (N = 14). The single plateau potential and BMP occurring at the end of the excerpt in D is illustrated for comparison with the B63 recording in A, but was not included in the spectral analyses of E (see ***Figure 2—figure supplement 1B***). In the absence of plateau potentials, the cells expressed spontaneous variations in membrane potential (**D**) composed of a single dominant, low-amplitude oscillation (**E,F**). Note that smaller additional peaks in the power spectra in **B,E** are essentially harmonics of the major period(s).

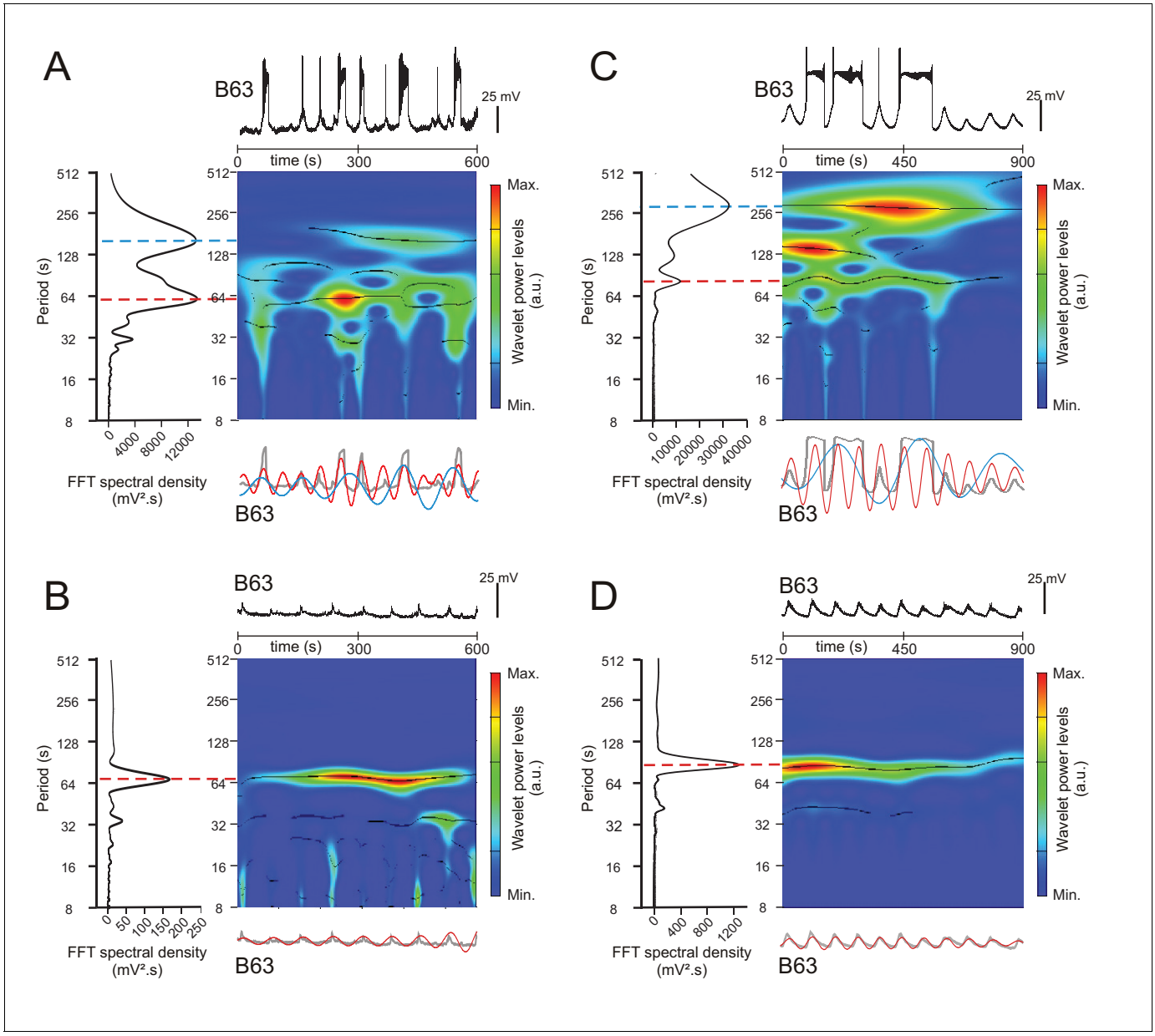

Figure 2—figure supplement 1. Spectral density analysis of B63 neuron intracellular recordings. (**A,B**) Analysis under normal saline (ASW) conditions. Colored panels (middle) are wavelet-based power spectral decompositions of the membrane potential variations over time in the B63 cell recording excerpt shown at top (Color code bars: power; black lines: ridges of power). Plots at left are periodograms from Fast Fourrier Transform (FFT) of the same intracellular recordings used to quantify spectral densities (i.e. amplitudes) at dominant periods (indicated by red and blue lines) of voltage changes in the period range between 8 and 512 s. Note that event period (in secs) rather than its reciprocal (frequency) was used in the time domain due to the very slow spontaneous rates of membrane potential fluctuations (see Materials and methods). Bottom traces are mathematically-reconstructed oscillations from the dominant periods revealed in the FFT periodograms (red and blue traces) superimposed with the corresponding intracellular recording excerpt after low pass filter smoothing to remove action potentials (gray traces). The recordings in A and B, and corresponding wavelet power spectra, periodograms and reconstructed oscillations, are from the same B63 neuron with (**A**) or without (**B**) the spontaneous expression of plateau potentials, as reported in ***Figure 2***. (**C,D**) Equivalent analysis under Low Ca+Co saline conditions to block chemical synapses. The intracellular recordings (Top traces) and corresponding wavelet and FFT power spectral decomposition and reconstructed waveforms are from the same B63 neuron with (**C**) or without (**D**) spontaneous plateau potential generation, as reported in ***Figure 3***.

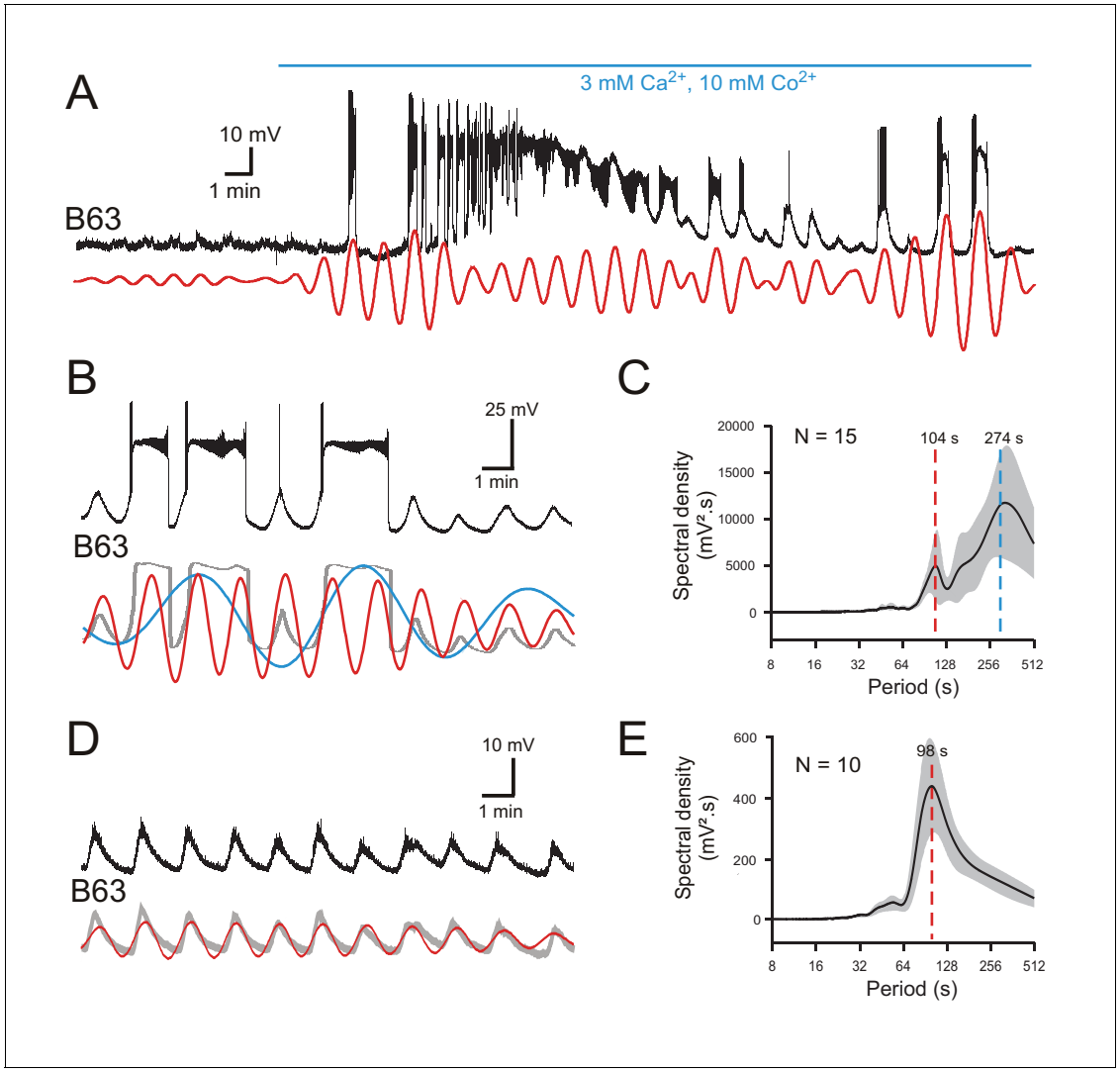

Figure 3. B63's voltage oscillations in the absence of functional chemical synapses. (**A**) Membrane potential fluctuations and plateauing in a recorded B63 neuron immediately before and during onset of bath-applied Low Ca+Co saline (horizontal blue line) to block chemical synapses in the buccal CPG network. Red trace: corresponding reconstructed waveform from the peak spectral density (period range: 70–90 s) (**B,C**) A different B63 cell recorded 20 min after onset of Low Ca+Co perfusion (B, Top trace; also see ***Figure 2—figure supplement 1C***). The membrane potential variations decomposed into two oscillatory waveforms (B, red and blue traces) with periods of 83 and 280 s, respectively. Gray trace: raw recording after smoothing. (**C**) Average power spectrum (mean period ± CI95%) from 15 neurons showing two major oscillations. (**D,E**) Same analysis as in B,C, but of B63 recording sequences without plateau potential generation (also see ***Figure 2—figure supplement 1D***). The remaining spontaneous variations in membrane potential now comprised a single oscillation (D, red trace: period 85 s), as also indicated by the solitary dominant period in the averaged periodogram (mean ± CI95%) from 10 B63 neurons (**E**).

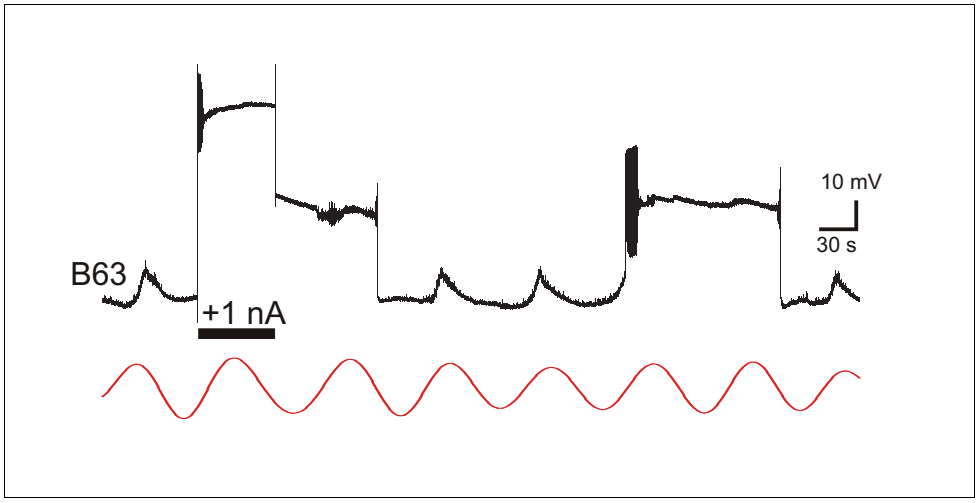

Figure 3—figure supplement 1. Expression of B63 plateau potentials with chemical synapses blocked
Intracellular recording of a B63 neuron in a buccal ganglion under bath-applied Low Ca+Co saline. A transient intracellular injection of depolarizing current (horizontal bar, +1nA) elicited a prolonged plateau potential that was similar to a subsequent plateau triggered spontaneously on a depolarizing phase of ongoing membrane potential oscillation. The red trace is the corresponding reconstructed waveform from the peak spectral density; period 71 s.

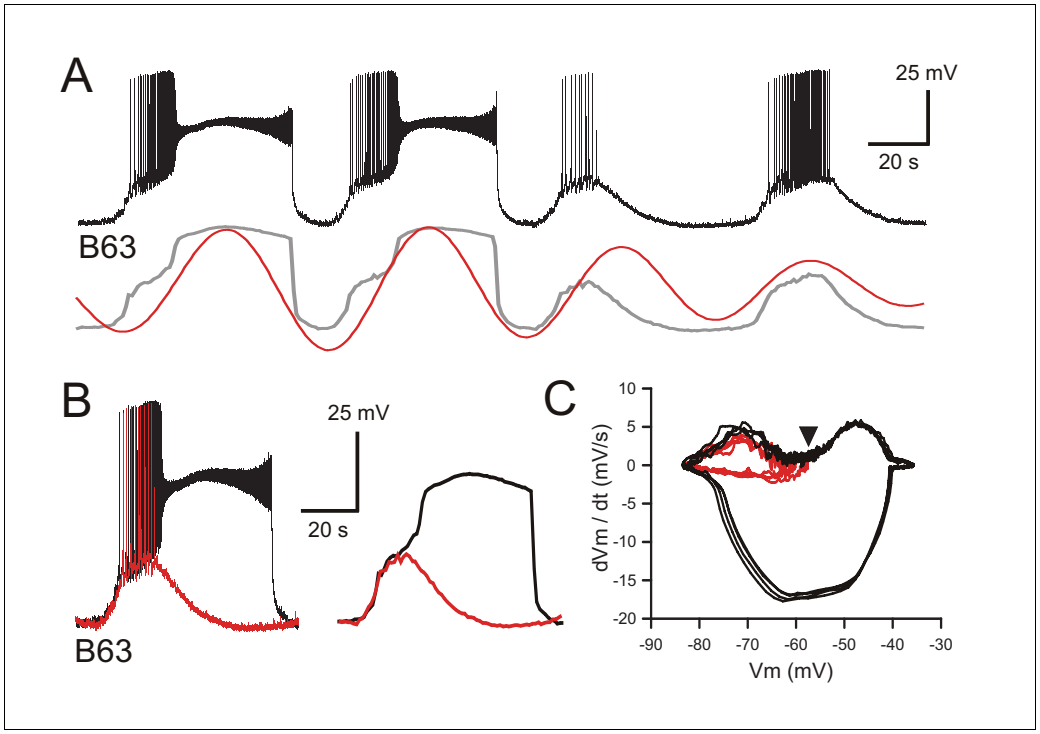

Figure 4. B63's voltage oscillation triggers plateau potentials. (**A**) Intracellular recording of a B63 neuron under chemical synapse blockade during an excerpt in which each spontaneous voltage oscillation was associated (first two cycles) or not (last two cycles) with the expression of plateau potentials. Bottom traces: corresponding smoothed recording (gray trace) and reconstructed oscillation from the peak spectral density (red trace; period 64 s). (**B**) Left: superposition of the first oscillation cycle in A with an accompanying plateau (black trace) and the third cycle without a plateau (red trace). Right: same traces after low-pass filtering to remove action potentials. (**C**) Phase-plane plot of 8 successive oscillation cycles both without (four cycles, red), and with (four cycles, black) plateau potential generation in the same B63 neuron as in **B, C**. The initial raising phases of the sub- and supra-threshold depolarizations follow identical trajectories before either a return to baseline potential or a further depolarization into a prolonged plateau. The arrowhead indicates the voltage threshold for plateau potential generation.

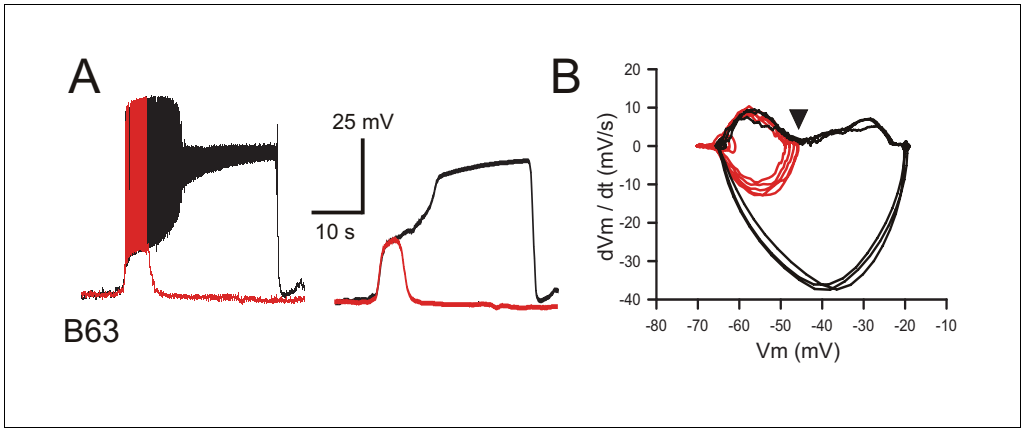

Figure 4—figure supplement 1. Triggering of plateau potentials by B63's voltage oscillation under normal saline (ASW) conditions. (**A**) Left: superposition of an oscillation cycle without a plateau (red trace) and one leading to a plateau (black trace) recorded in the absence of chemical synapse blockade. Right: same traces after low-pass filtering to remove action potentials. (**B**) Phase-plane plot of 8 successive oscillation cycles both without (five cycles; red), and with (three cycles; black) plateau potential generation in the same B63 neuron. The arrowhead indicates the voltage threshold for plateau potential generation.

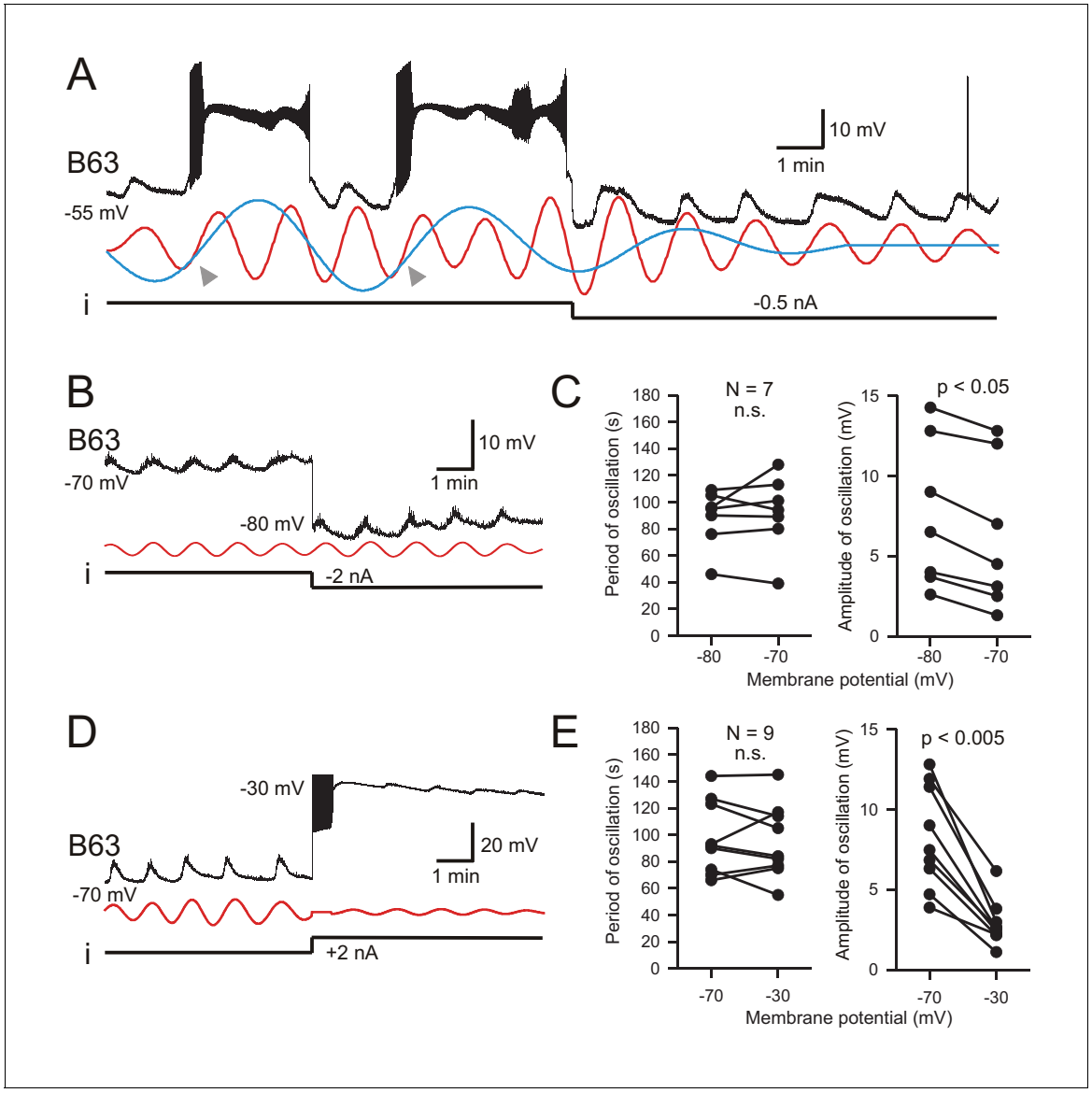

Figure 5. B63's low-amplitude oscillation does not arise from a voltage-sensitive mechanism. (**A**) Under chemical synapse blockade (with Low Ca+Co saline), a B63 neuron's spontaneous plateau potentials, but not its low-amplitude voltage oscillation, are suppressed by continuous hyperpolarizing current injection (i, −0.5 nA). Red and blue traces: superimposed reconstructed waveforms from the peak spectral densities corresponding to the presence or absence of plateau potentials. Arrowheads indicate the points of waveform intersection where plateau potentials were initiated. (**B**) Low-amplitude oscillation (upper trace) in a different B63 neuron during continuous hyperpolarization with chemical synapses blocked. The cell's membrane potential was held at −70 mV then stepped to −80 mV by continuous intracellular current injection (i) with two-electrode current clamp. Red trace: reconstructed waveform from the peak spectral density (period 80 s). (**C**) The oscillation cycle periods of all seven recorded neurons (left) were not significantly (n.s.) modified by the same membrane potential manipulation (V = 16, p = 0.799). However, this hyperpolarization significantly increased the oscillation amplitude (right, V = 0, p = 0.012). (**D,E**) Same analysis as in B,C, but with the membrane potential initially held at −70, then depolarized to −30 mV with two-electrode current clamp (**D**). Red trace: reconstructed waveform from the peak spectral density (period: 70 s). (**E**) No significant difference (n.s.) in oscillation period (left) was found in nine recorded neurons at these two holding potentials (V = 28, p = 0.553), whereas the depolarization caused a significant decrease in oscillation amplitude (right, V = 45, p = 0.0039).

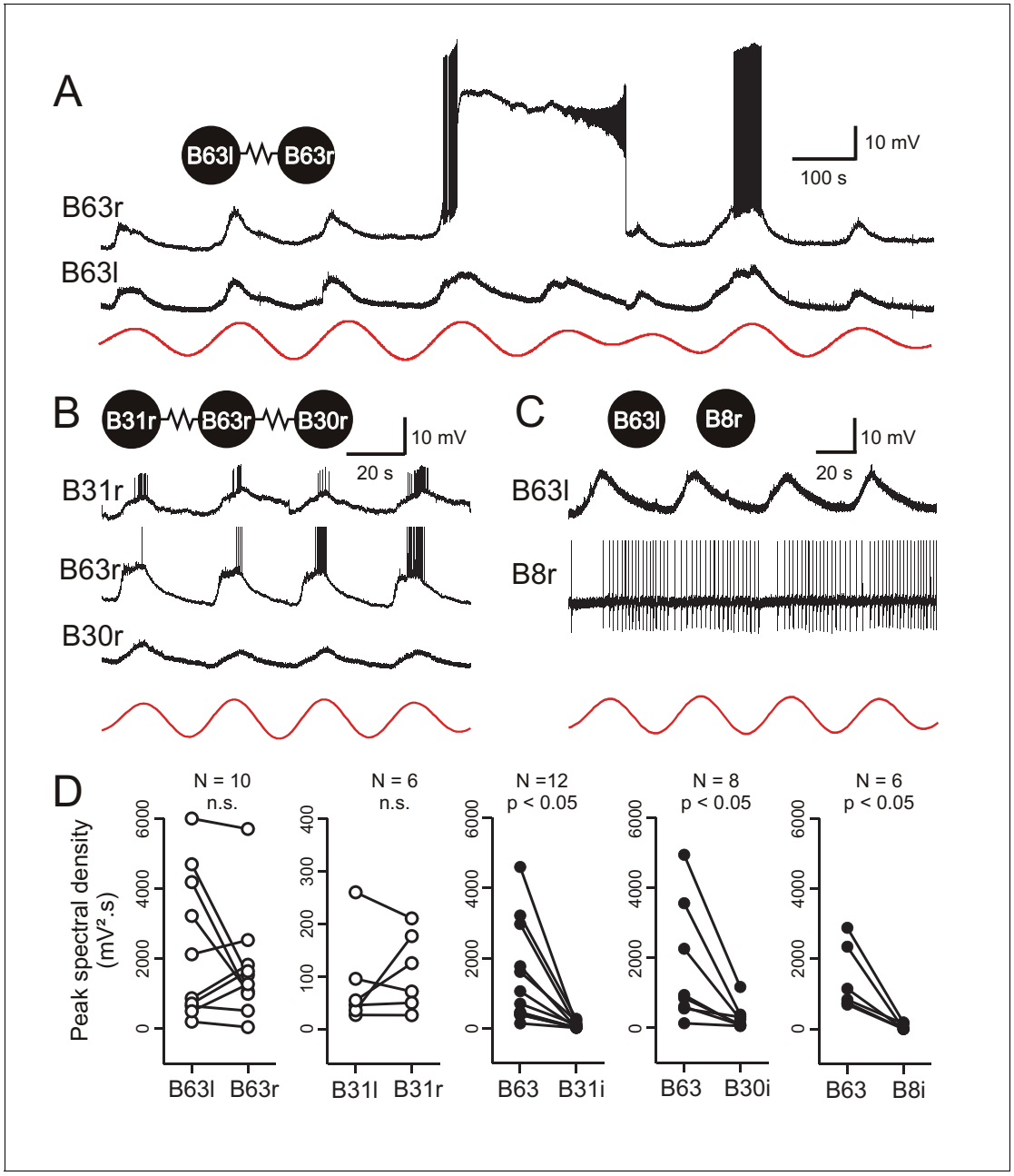

Figure 6. Low-amplitude oscillation in electrically-coupled network neurons. (**A,B**) Simultaneous intracellular recordings from different protraction generator neurons under chemical synapse blockade. (**A**) Spontaneous membrane potential oscillations in the right (r) and left (l) electrically coupled B63 cells (resistance symbol: electrical synapse). Note the independent expression of a plateau potential and burst firing in B63r. (**B**) Coordinated oscillations in a right B63 and ipsilateral, electrically coupled B31 and B30 neurons (the action potentials in the B63 trace are truncated). Red traces in A and B: reconstructed waveforms from the peak spectral densities for B63l and B63r, respectively. (**C**) Simultaneous intracellular recordings from a B63 cell and a non-coupled contralateral B8 motor neuron (action potentials in the B8 trace are truncated). A membrane voltage oscillation was absent in B8. Red trace: reconstructed waveform from the peak spectral density for B63. (**D**) Comparison of oscillation magnitude (i.e., peak spectral amplitude) in contralateral (unfilled dots; l, left; r, right) and ipsilateral neurons (i, filled dots). The oscillation amplitude was not significantly different (n.s.) in bilateral homologous cells (white dots; B63r/B63l, V = 22, p = 0.625; B31r/B31l, V = 13, p = 0.688), but was significantly higher in B63 compared to heterologous neurons in the same (i, ipsilateral) ganglion (black dots; B63/B31i, V = 78, p = 0.005; B63/B30i, V = 36, p = 0.008; B63/B8i, V = 21, p = 0.031).

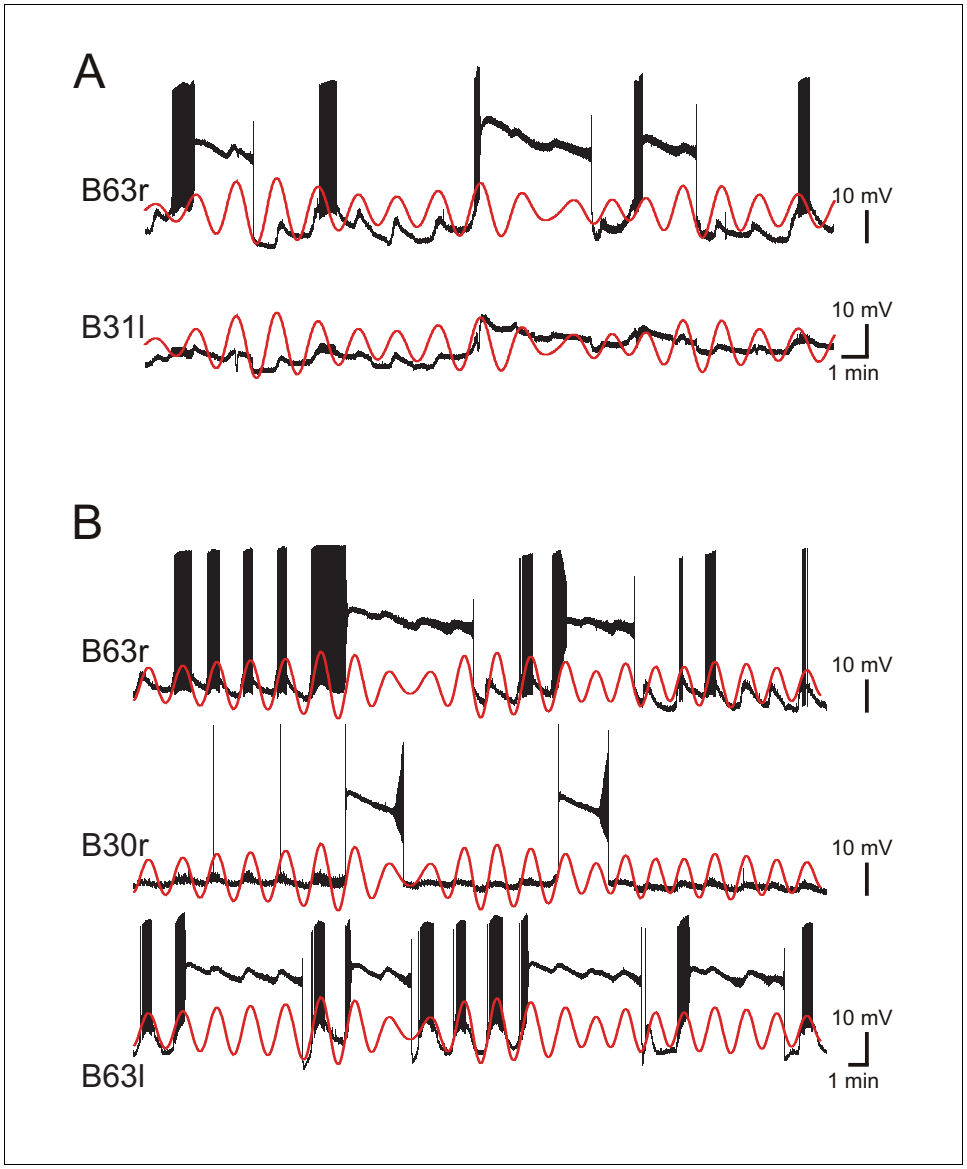

Figure 6—figure supplement 1. Irregular plateau potentials triggered by regular voltage oscillations in electrically coupled network neurons. (**A**) Paired intracellular recordings from two gap junction-coupled neurons (right B63 and left B31) under chemical synapse blockade. In contrast to the continuous synchronous and rhythmic depolarizations (see red traces, which are the reconstructed voltage oscillation of B63 superimposed with both the raw B63 and B31 recordings), the production of plateau potentials was irregular and occurred independently in the two neurons. (**B**) Simultaneous recordings from three gap junction-coupled neurons (right B63, right B30, and left B63) under chemical synapse blockade. All three cells expressed synchronous, rhythmic depolarizations (red traces: reconstructed voltage oscillation of right B63 superimposed with all raw recordings), but again, the onsets and terminations of plateau potentials were highly irregular within and between the individual neurons.

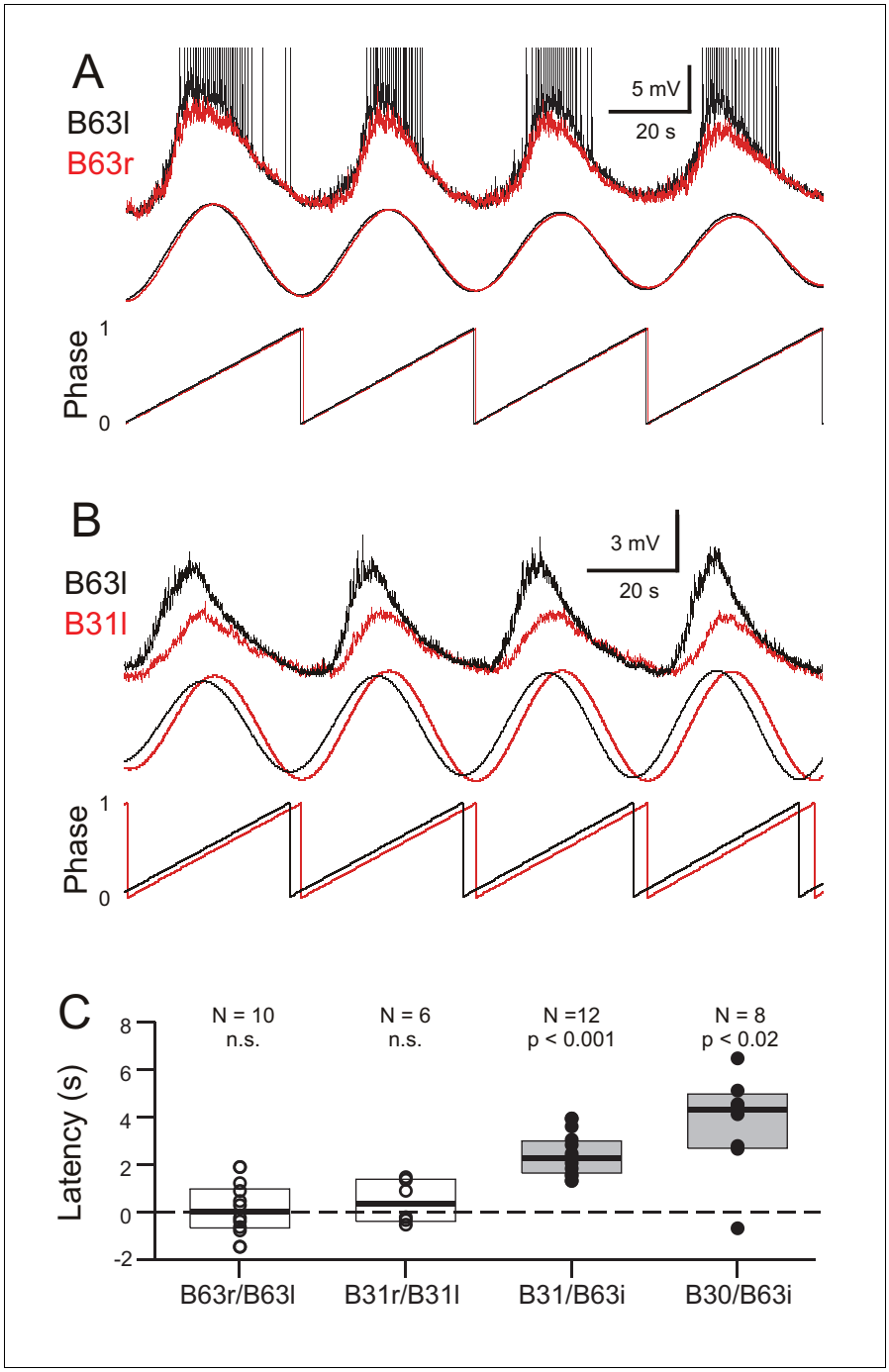

Figure 7. Phase-relationships between the oscillations of different network neurons. (**A**,**B**) Upper traces: Superimposed phase-aligned intracellular recordings from different neuronal pairs – (**A**), left (black) and right B63 (red); (**B**), left B63 (black) and left B31 (red) – under chemical synapse blockade (action potentials in B63l are truncated). Middle traces, reconstructed waveforms from the corresponding spectral periodograms after equivalence amplitude scaling. Lower traces: superimposed representations of the oscillation phases in each cell pair. No phase difference was evident between the two B63 neurons (**A**). In contrast, the oscillation of B63 (black) was phase-advanced relative to that of B31 (**B**). (**C**) One-sample analyses showing that the oscillation latencies in homologous bilateral neurons were not significantly (n.s.) different from zero (unfilled dots and boxes; B63r/B63l, $V_0 = 31$, $p = 0.770$; B31r/B31l, $V_0 = 15$, $p = 0.438$). In contrast, oscillations in heterologous neurons were significantly delayed (i.e. positive latency) relative to the ipsilateral (i) B63 partner (filled dots and boxes; B31/B63i, $V_0 = 78$, $p = 0.0005$; B30/B63i, $V_0 = 35$, $p = 0.016$).

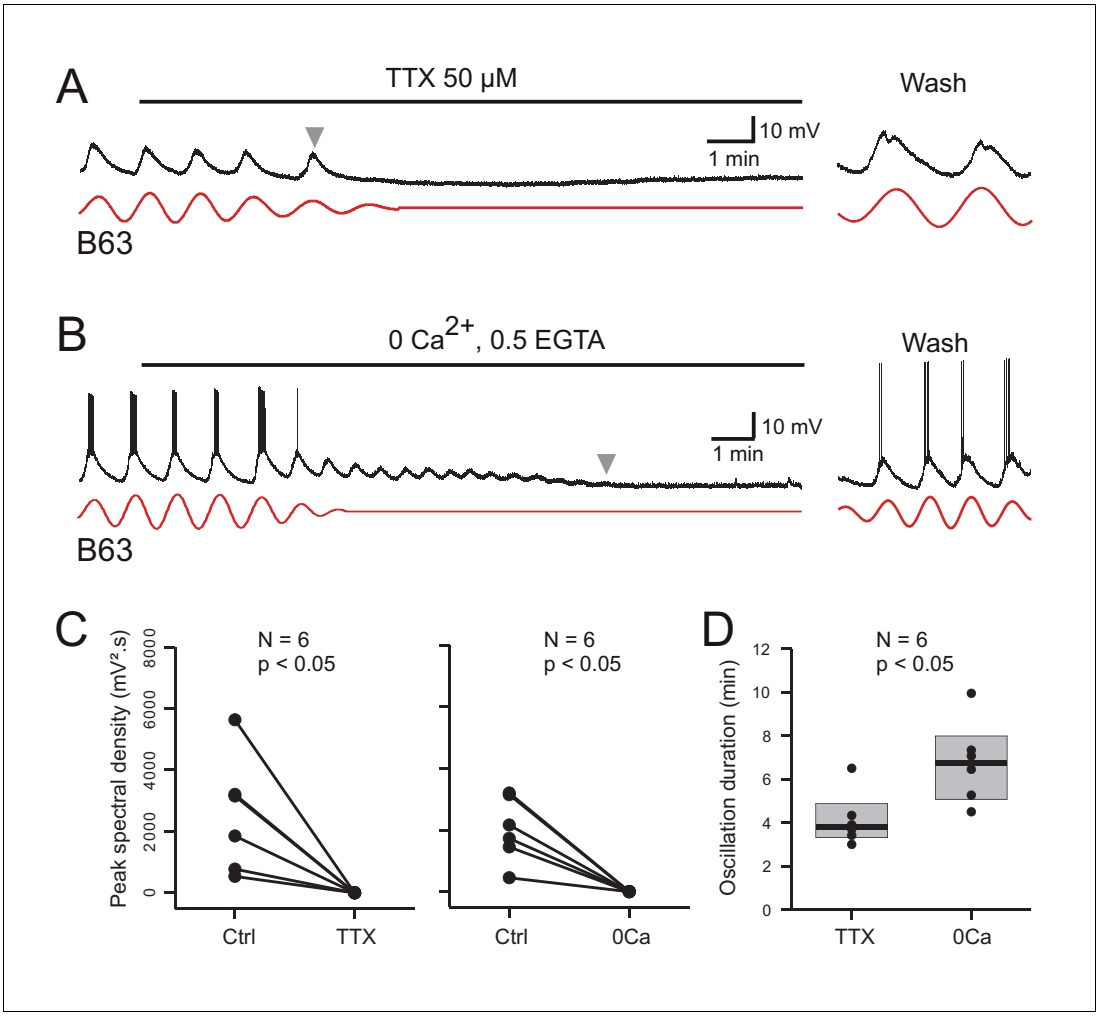

Figure 8. Involvement of sodium and calcium ions in the voltage oscillation. (**A**,**B**) Under chemical synapse blockade, the spontaneous voltage oscillations of B63 neurons were reversibly (trace excerpts at right) suppressed by bath application of 50 µM tetrodotoxin (A, horizontal line), or calcium-free salines (B, horizontal line). Red traces: reconstructed waveforms from corresponding peak spectral densities. (**C**) Group quantification under the experimental conditions illustrated in A,B: The amplitude of the dominant oscillation in Low Ca+Co saline alone (Control, Ctrl) was significantly reduced after application of TTX-containing (left, V = −21, p = 0.031), or calcium-free saline (right, V = −21, p = 0.031). (**D**) Inter-group comparison of oscillation longevity (gray arrowheads in A-C) after modified-saline perfusion onset (W = 3, p < 0.015). B63's oscillation persisted for significantly longer after removal of extracellular calcium (0 Ca + 0.5 EGTA) than after blockade of sodium channels by TTX.

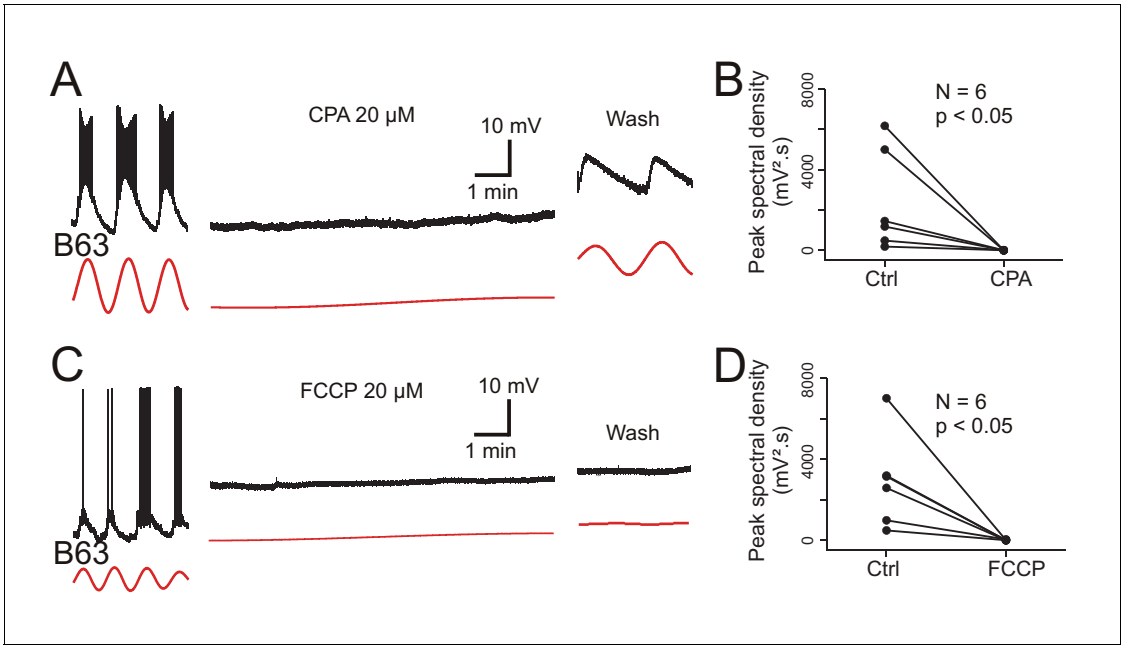

Figure 9. Involvement of intracellular calcium stores in the voltage oscillation. (**A**) The spontaneous voltage oscillation of a B63 neuron (left excerpt) was reversibly (right excerpt) suppressed in the presence of 20 µM CPA, a SERCA inhibitor (middle excerpt, recorded 20 min after the beginning of drug application). (**B**) Group analysis showing a significant reduction in oscillation magnitude of 6 B63 neurons measured before (Ctrl) and 20 min after the beginning of CPA application (V = 21, p = 0.031). (**C**) Suppression of B63 oscillation by application of 20 µM FCCP, an uncoupler of mitochondrial oxidative phosphorylation leading to calcium release. The neuron's spontaneous oscillation (left) was irreversibly (right) suppressed and the cell depolarized (middle, recorded 20 min after the beginning of drug application). (**D**) The oscillation magnitudes (Ctrl) of 6 tested B63 neurons were significantly reduced (V = 21, p = 0.031) after 20 min of FCCP application.

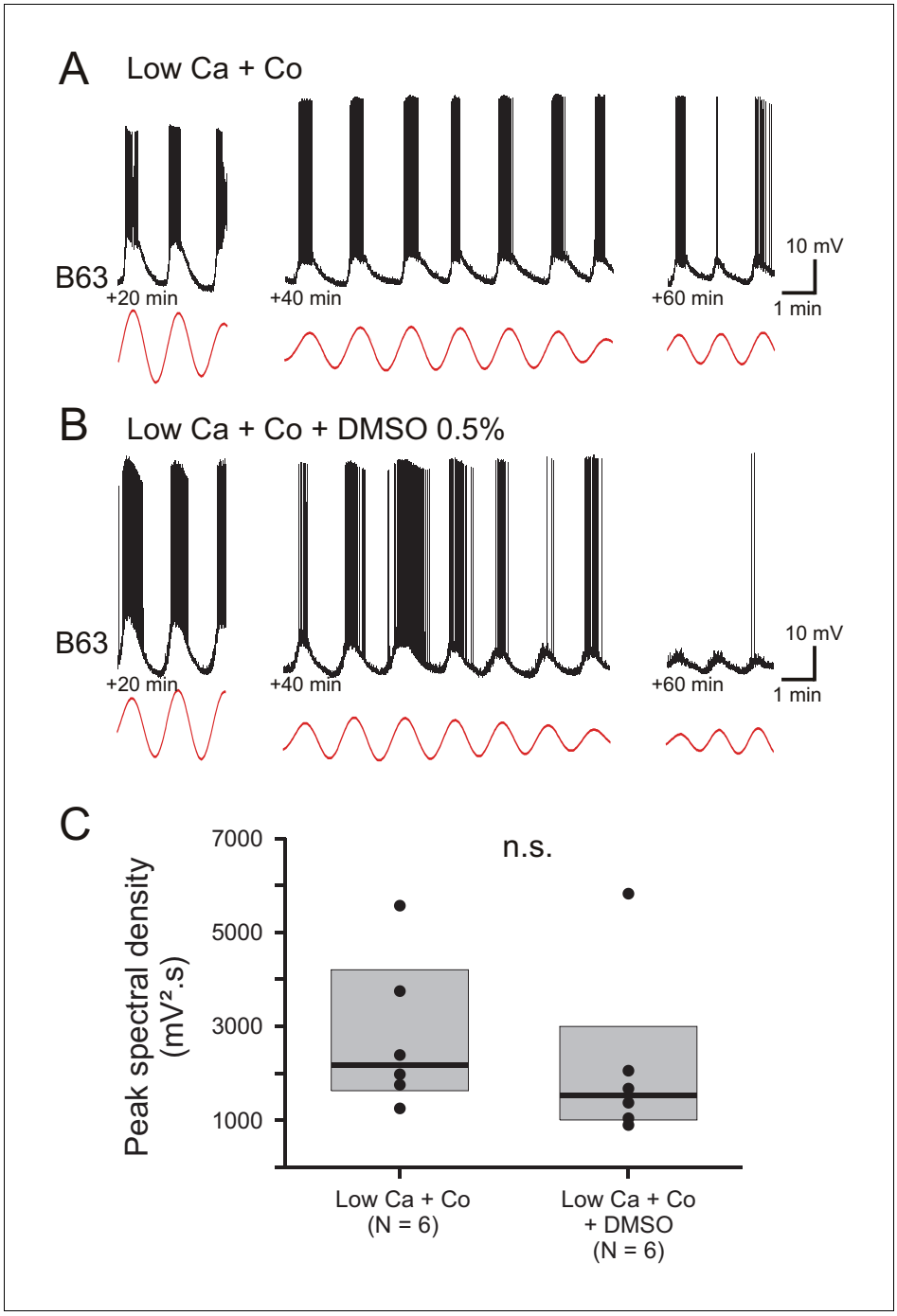

Figure 9—figure supplement 1. The voltage oscillation of B63 is unaffected by exposure to DMSO. (**A**,**B**) Recordings from two different B63 neurons during bath-application of Low Ca+Co saline alone (**A**) or additionally containing 0.5% DMSO (**B**). Left trace excerpts: 20 min after the beginning of the perfusion. Middle traces: 40 min after perfusion onset. Right traces: 60 min after perfusion onset. Red traces: reconstructed waveforms from the corresponding peak spectral densities. (**C**) Group comparison of oscillation magnitudes in B63 cells measured from 20 until 30 min after the beginning of saline perfusion in the absence (left) and presence of 0.5% DMSO (right). DMSO had no significant (n.s.) effect on the amplitudes of the voltage oscillations (Mann-Whitney rank sum test: V = 25, p = 0.310).

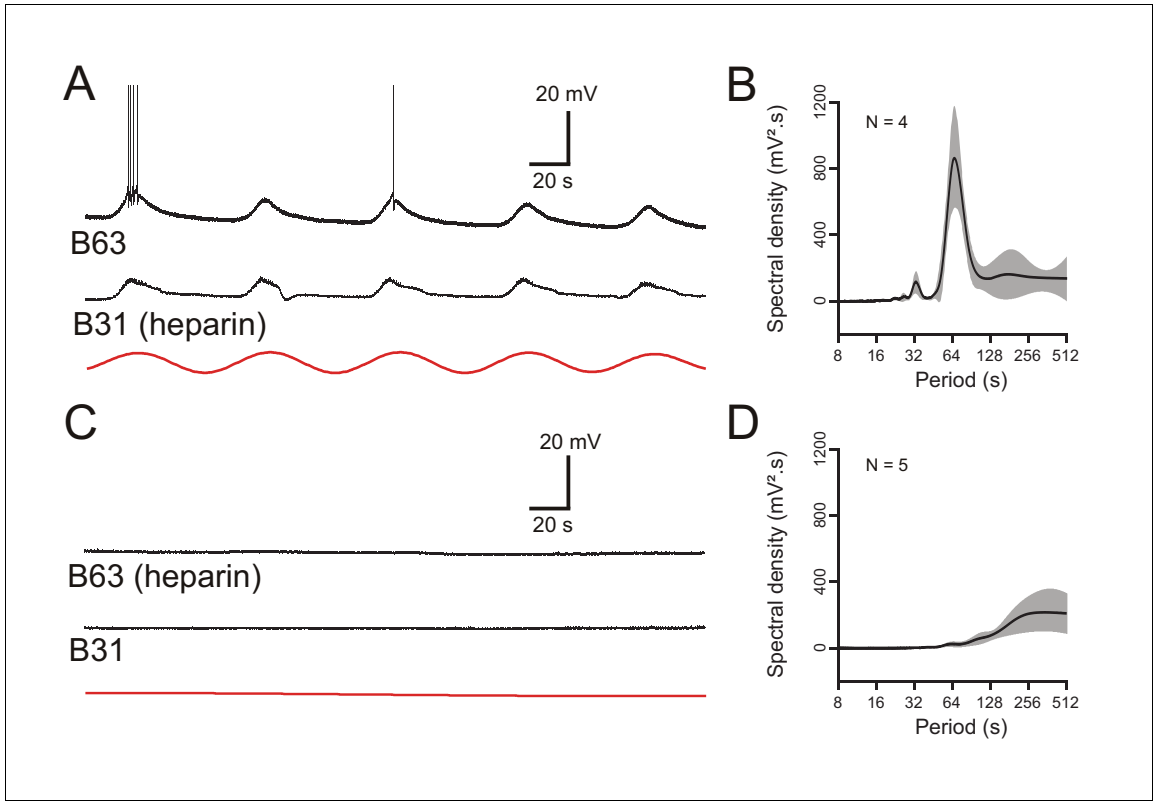

Figure 10. The voltage oscillation generated by intracellular calcium store release is specific to B63. (**A,C**) Paired recordings of B63 and B31 neurons under chemical synapse blockade, 30 min after the beginning of an intrasomatic injection of the ER membrane calcium channel blocker heparin (20 mg/ml) into either the bilateral B31 (**A**) or bilateral B63 (**C**) neurons. Heparin in B31 had no effect on the ongoing oscillation of an un-injected B63 cell (**A**), but suppressed oscillations in both a B63 and an un-injected B31 (**C**) after injection into both B63 neurons. Red traces: reconstructed waveforms from the corresponding periodograms. (**B,D**) Average power spectra obtained 30 min after the beginning of bilateral intracellular heparin injection into the B31 (**B**) or B63 neurons (**D**) in 4 and 5 preparations, respectively.